American Journal of Electrical and Computer Engineering
2026; 10(1): 19-34
http://www.sciencepublishinggroup.com/j/ajece
doi: 10.11648/j.ajece.20261001.12

Optimal Load Frequency Control of an Isolated Multi Source Power System Using Sailfish Optimization Algorithm

Shuhangi Sambariya*, Mahendra Lalwani, Dhanesh Kumar Sambariya

Department of Electrical Engineering, Rajasthan Technical University, Kota, India

Email address:
ssambariya@yahoo.com (Shuhangi Sambariya), mlalwani@rtu.ac.in (Mahendra Lalwani),
dksambariya@rtu.ac.in (Dhanesh Kumar Sambariya)

To cite this article:
Shuhangi Sambariya, Mahendra Lalwani, Dhanesh Kumar Sambariya. (2026). Optimal Load Frequency Control of an Isolated Multi Source Power System Using Sailfish Optimization Algorithm. *American Journal of Electrical and Computer Engineering, 10*(1), 19-34.
https://doi.org/10.11648/j.ajece.20261001.12

Received: 14 June 2026; **Accepted:** 22 July 2026 **Published:** 25 August 2026

Abstract: Load Frequency Control (LFC) plays a vital role in maintaining the stability, reliability, and quality of power system operation by regulating system frequency and balancing generation with load demand. This paper investigates the LFC problem for an isolated multi-source power system comprising Thermal, Hydro, and Gas power generation units. To achieve effective frequency regulation under load disturbances, a decentralized control strategy employing three Proportional-Integral (PI) controllers is adopted. Among these, one PI controller is commonly shared by all generating units, while the remaining two controllers are independently assigned to the Thermal and Gas generating units to improve their dynamic response. The optimal tuning of the PI controller parameters is formulated as an optimization problem and solved using the Sailfish Optimization (SFO) algorithm, a recent nature-inspired metaheuristic optimization technique known for its excellent exploration and exploitation capabilities. The Integral Square Error (ISE) is selected as the objective function to minimize frequency deviations and enhance the overall dynamic performance of the power system. The effectiveness of the proposed SFO-based PI controller is evaluated through comprehensive time-domain simulations under step load perturbations. The system performance is assessed using transient response characteristics, including maximum overshoot, rise time, settling time,together with standard performance indices and eigenvalue analysis to examine system stability. The simulation results demonstrate that the proposed SFO-PI controller significantly improves frequency regulation, reduces oscillations, and achieves faster settling with lower performance index values compared with conventional PI tuning approaches and other optimization-based controllers reported in the literature. Furthermore, eigenvalue analysis confirms enhanced damping characteristics and improved stability of the proposed control scheme. The results establish that the SFO provides an effective and reliable framework for optimal controller design in isolated multi-source power systems.

Keywords: Isolated Multi Source Power System, Load Frequency Control, Sailfish Optimization Algorithm, PI Controller, Integral Square Error

1. Introduction

Load frequency control (LFC) is a critical component of the automatic generation control (AGC) scheme in power systems, playing a vital role in maintaining system stability and reliability. As one of the primary control procedures, LFC addresses the challenge of frequency deviations caused by imbalances between power generation and demand. These deviations, if left unchecked, can lead to severe consequences, ranging from partial load shedding to complete blackouts. The reliability of an electrical power system hinges on its ability to maintain frequency close to its nominal value, making LFC a long standing and essential research topic in power system operation [1, 2]. In interconnected systems, LFC not only stabilizes frequency but also ensures that power exchange between areas remains within predefined limits. Over the decades, researchers have explored various approaches to enhance LFC performance, aiming to maintain frequency and

AC voltage levels despite disturbances [3].

The power generation system studied in this paper has been extensively analysed in prior research, with a focus on optimizing controller performance using diverse algorithms and objective functions. For instance, genetic algorithms (GA) have been employed to tune PI controllers, comparing centralized and decentralized control strategies[4]. Other studies have utilized optimization techniques such as the water cycle algorithm (WCA) [5], grey wolf optimization (GWO) [6], differential evolution (DE), and teaching-learning-based optimization (TLBO) [7]. Additionally, various controller types [8], including PID Ziegler-Nichols, PID Chien-Hrones-Reswick, and fuzzy PID, have been evaluated [9]. Stochastic fractal search (SFS), local unimodal sampling (LUS), and particle swarm optimization (PSO) have also been applied to tune PID controllers [10]. Furthermore, research has extended to interconnected power systems, incorporating plug-in electric vehicles (PEVs) and comparing algorithms such as modified grey wolf optimization (mGWO) and hybrid stochastic fractal search (hSFS) [11].

In recent years, metaheuristic optimization methods have gained prominence over traditional techniques due to their simplicity and effectiveness. Among these, swarm-based bio-inspired algorithms have demonstrated remarkable success in solving complex optimization problems.

The key contributions of this study are as follows:

1) A comprehensive analysis of the dynamic behaviour of a realistic single-area multi-source power generation system.
2) The application of the SFO algorithm to optimize PI controllers for LFC, addressing a gap in existing research.
3) A comparative evaluation of SFO against PI controller design by Ramakrishna and Bhatti [4].

Frequency stability is a cornerstone of power system quality, and LFC serves as the primary mechanism to mitigate frequency variations. The inclusion of a secondary controller is essential for achieving optimal performance and restoring power supply to desired levels [3, 11]. However, the effectiveness of secondary controllers depends heavily on the optimization of their gains. This study leveraged advanced optimization strategy, informed by extensive literature review, to enhance controller performance.

2. Multi-source Power Generating System Under Study

2.1. System Overview

In this study, Load Frequency Control (LFC) is analyzed for an isolated multi-source power system. The considered system comprises three distinct power generation sources: a reheated thermal-turbine, a hydro-turbine, and a gas-turbine. The block diagram for the considered system is presented in Figure 1. It is observed that in normal operating conditions, the power generation and demand remain balanced, subjected to following relationship in Eq. 1 holds as in Karnavas and Nivolianiti [12].

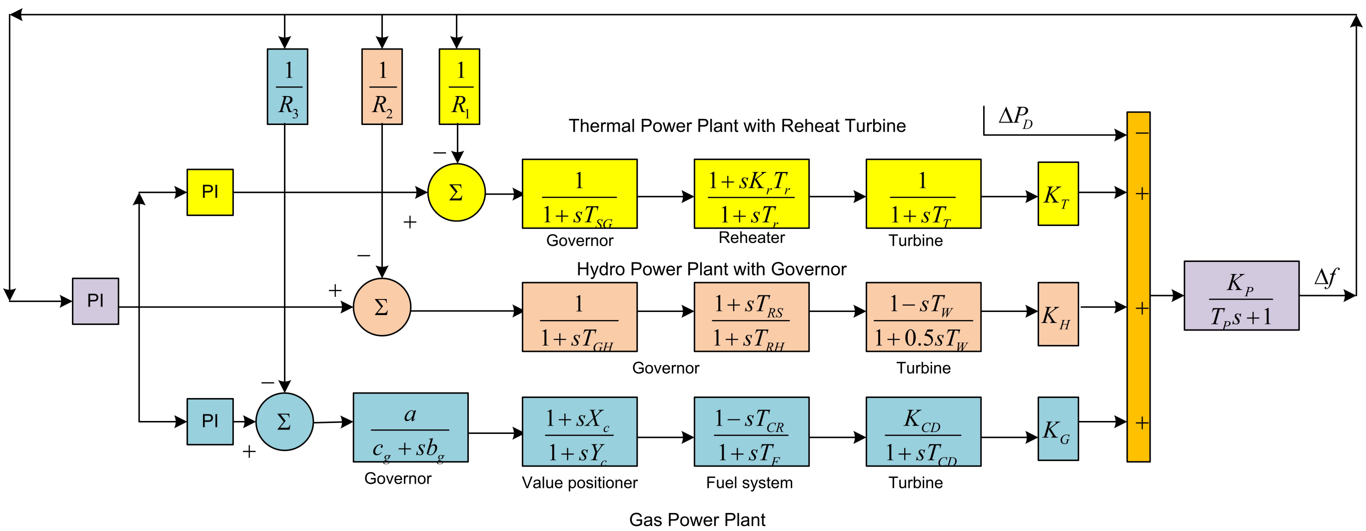

Figure 1. *Basic model of single-area load frequency control.*

$$P_G = P_{Gs} + P_{Gh} + P_{Gg} \tag{1}$$

where P_{Gs}, P_{Gh} and P_{Gg} represents power of the thermal, hydro and gas power generation source, respectively. However, the power generated by the sources includes the vital role of source participation factor where K_T, K_H and K_G represents participation value of thermal, hydro and gas plants, respectively. It is also detrimental that the submission of all participation factors must be equal to unity as in Eq. 2.

$$K_T + K_H + K_G = 1.0 \quad (2)$$

In this system the total power generated is assumed as $1750MW$ which comprises $1000MW$, $500MW$ and $250MW$ from thermal, hydro and gas generating sources, respectively. On the other hand the participation factors are $K_T = 0.57143$, $K_H = 0.28571$ and $K_G = 0.14286$ [2].

The power demand ΔP_D which must be covered by the generating sources.The change in frequency Δf is the difference of generated and demand power and can be represented by the following relationship, Eq. 3:

$$\Delta P_G(s) + \Delta P_{Gh}(s) + \Delta P_{Gg}(s) - \Delta P_D(s) = \frac{2H}{f_0}\Delta f(s) + D\Delta f(s) \quad (3)$$

The relationship between change in frequency and generated power can be represented by following transfer function:

$$\frac{\Delta f(s)}{\Delta P_G(s)} = \frac{K_p}{sT_p + 1} \quad (4)$$

The power system gain constant K_p (in Hz/pu MW)and power system time constant, T_p can be represented by following expresion Eq. 5:

$$T_{ps} = \frac{2H}{f_0 D}$$
$$K_p = \frac{1}{D} \quad (5)$$

where system inertia constant is H, the damping factor is D and f_0 is the system rated frequency.

2.1.1. Steam Generation Source

Considering Figure 1, the output of the speed governor is given by expression in Eq. 6. Where K_{SG} and T_{SG} represents gain and time constant of steam turbine governor.

$$\frac{\Delta P_{sg}(s)}{\Delta P_s(s) - \frac{\Delta f(s)}{R_s}} = \frac{K_{SG}}{T_{SG}s + 1} \quad (6)$$

The subsystem of re-heater can be represented by following expression:

$$\frac{\Delta P_r(s)}{\Delta P_{sg}(s)} = \frac{K_r T_r s + 1}{T_r s + 1} \quad (7)$$

where, K_r and T_r represents the gain and time constant of re-heater. The output signal of turbine can be represented by following expression Eq. 8:

$$\frac{\Delta P_{st}(s)}{\Delta P_r(s)} = \frac{K_T}{T_T s + 1} \quad (8)$$

where K_T and T_T are gain and time constants of the steam turbine.

2.1.2. Hydro Generation Source

The first two blocks of the system shown in Figure 1 represents operation of a mechanical-hydrolic speed governor. One of the blocks represents motor pilote stage that drives the second block which controls the water intake walve on equilibrium position of generated power and demand, the power flow is constant while on disturbance the speed controller reacts to restore balance. Therefore, the system transfer function for speed governor can be represented as following:

$$\frac{\Delta P_{hg}(s)}{\Delta P_h(s) - \frac{\Delta f(s)}{R_h}} = \frac{1}{1 + sT_{GH}} \frac{1 + sT_{RS}}{1 + sT_{RH}} \quad (9)$$

The output of mechanical-hydraulic governor $\Delta P_{hg}(s)$ is a function of $\Delta P_h(s)$ and $\Delta f(s)/R_h$. The T_{RS}, T_{RH} and T_{GH} are hydro turbine speed reset time, transient droop time constant and servo time constant, respectively. The block which represents mechanical input power to electrical output power is represented as following as in Eq. 10:

$$\frac{\Delta P_{ht}(s)}{\Delta P_{hg}(s)} = \frac{-T_w s + 1}{0.5T_w s + 1} \quad (10)$$

where T_w is penstock water time constant.

2.1.3. Gas Generation Source

The output of the speed controller in gas turbine power plant shwon in Figure 1 is a function of the corrective action represented as following:

$$\frac{\Delta P_{gg}(s)}{\Delta P_g(s) - \frac{\Delta f(s)}{R_g}} = \frac{sX_c + 1}{sY_c + 1} \quad (11)$$

where gas turbine speed governor lead time and lag time are represented by X_c and Y_c respectively.

The secondary stage control valve positioner sub system is represented as following:

$$\frac{\Delta P_{vp}(s)}{\Delta P_{gg}(s)} = \frac{a}{bs + c} \quad (12)$$

where a ,c are the gain constants of the valve positioner and b is the time constant of the valve positioner.

The fuel and combustion sub-system where chemical reaction takes place resulting to thermal energy generation is represented as following:

$$\frac{\Delta P_{fc}(s)}{\Delta P_{vp}(s)} = \frac{1 - T_{cr}s}{T_f s + 1} \quad (13)$$

where combustion chamber time delay and fuel time constant are represented by T_{cr} and T_f respectively. The last stage in the gas system is represented as following:

$$\frac{\Delta P_{gt}(s)}{\Delta P_{fc}(s)} = \frac{K_{CD}}{T_{CD}s + 1} \quad (14)$$

where compressor discharge volume coffecient and time constant are represented by $K_C D$ and $T_C D$, respectively.

2.2. PI Controller

The PI controller is described by the well-known transfer function:

$$G_{PI}(s) = K_p + \frac{K_i}{s} \tag{15}$$

where K_p is the proportional gain and K_i is the integral gain. The PI parameters are to be optimized through SFO algorithm under following constraints:

$$K_P^{\min} \leq K_p \leq K_P^{\max} \tag{16}$$

$$K_i^{\min} \leq K_i \leq K_i^{\max} \tag{17}$$

2.3. Objective Function

In the optimization process, the proportional-integral (PI) controller parameters are optimized by minimizing different performance index-based objective functions. These objective functions quantify the system error and are widely employed to evaluate the dynamic performance of load frequency control (LFC) systems. Let the error signal be defined as

$$e(t) = \Delta f(t) \tag{18}$$

where $e(t)$ denotes the frequency deviation (error) at time t, and T represents the total simulation time. The performance indices considered in this study are described as follows.

1) *Integral Absolute Error (IAE)*
The IAE minimizes the accumulated absolute value of the error over the simulation period and is expressed as

$$J_{\text{IAE}} = \int_0^T |e(t)|\, dt \tag{19}$$

2) *Integral Square Error (ISE)*
The ISE emphasizes larger errors by squaring the error signal and is given by

$$J_{\text{ISE}} = \int_0^T e^2(t)\, dt \tag{20}$$

3) *Integral Time Absolute Error (ITAE)*
The ITAE assigns a higher penalty to errors that persist for a longer duration and is defined as

$$J_{\text{ITAE}} = \int_0^T t\,|e(t)|\, dt \tag{21}$$

4) *Integral Time Square Error (ITSE)*
The ITSE penalizes large errors occurring at later stages of the response and is expressed as

$$J_{\text{ITSE}} = \int_0^T t\, e^2(t)\, dt \tag{22}$$

5) *Integral Time Cubed Error (ITCE)*
The ITCE provides a stronger penalty for errors that persist over time by introducing a higher-order time weighting and is defined as

$$J_{\text{ITCE}} = \int_0^T t^2 e^2(t)\, dt \tag{23}$$

6) *Root Mean Square Error (RMSE)*
The RMSE measures the root mean square value of the error throughout the simulation interval and is given by

$$J_{\text{RMSE}} = \sqrt{\frac{1}{T}\int_0^T e^2(t)\, dt} \tag{24}$$

Among these objective functions, IAE, ISE, ITAE, ITSE, ITCE, and RMSE were independently employed to optimize the PI controller parameters using the proposed SFO algorithm. The optimized controller parameters obtained using each objective function are to be compared to identify the performance index that provides the best dynamic response for the considered load frequency control system.

3. Sailfish optimization Algorithm

Group hunting is a remarkable social behaviour observed in various animal species, including arthropods, fishes, birds, and mammals, where cooperative hunting enables predators to capture prey with less individual effort than solitary hunting. Such hunting strategies range from simple, uncoordinated attacks to highly organized behaviours in which predators assume specialized roles. One of the most sophisticated strategies is attack alternation, wherein predators conserve energy while other members of the group repeatedly attack and weaken the prey. Sailfish, recognized as the fastest fish in the ocean, exhibit this behaviour while hunting sardine schools. During the hunt, sailfish alternately attack the sardines, inflicting injuries that gradually isolate individual prey from the school. Although sardines possess considerable agility, they are often unable to evade the rapid strikes of sailfish. The injured sardines become separated from the group, making them more vulnerable to predation [13]. While most individual attacks do not result in immediate capture, repeated strikes progressively weaken the sardines, ultimately leading to successful predation. Sailfish also display distinctive behaviour, such as erecting their dorsal fins for enhanced stability and changing body colour, which may facilitate communication and coordination during group hunting. Inspired by these cooperative hunting mechanisms, the SFO algorithm mathematically models the interaction between sailfish and sardines to solve complex optimization problems efficiently by Shadravan et al.[14].

3.1. Initialization

The SFO algorithm is a population-based meta-heuristic optimization technique inspired by the cooperative hunting behaviour of sailfish. In SFO, each sailfish represents a candidate solution, while the decision variables of the optimization problem correspond to the position of the sailfish within the search space. The algorithm begins by randomly initializing a population of sailfish over the feasible solution domain. Depending on the complexity of the optimization problem, sailfish can search in one-dimensional, two-dimensional, three-dimensional, or higher-dimensional spaces, with their positions represented by variable vectors [13]. In a d-dimensional search space, the position of the i^{th} sailfish at the k^{th} iteration is denoted by $SF_{i,k} \in R$, where $i = 1, 2, \ldots, m$, and m is the total number of sailfish. The positions of all sailfish are stored in a matrix, SF, where each row corresponds to a candidate solution and collectively represents the population employed throughout the optimization process [14].

The positions of all sailfish in the population are stored in a position matrix, where each row represents a candidate solution and each column corresponds to a decision variable. The sailfish position matrix is defined as

$$SF_{position} = \begin{bmatrix} SF_{1,1} & SF_{1,2} & \ldots & SF_{1,d} \\ SF_{2,1} & SF_{2,1} & \ldots & SF_{2,d} \\ \vdots & \vdots & \vdots & \vdots \\ SF_{m,1} & SF_{m,1} & \ldots & SF_{m,d} \end{bmatrix} \tag{25}$$

where m denotes the total number of sailfish in the population and d represents the number of decision variables of the optimization problem. The element $SF_{i,j}$ corresponds to the value of the j^{th} decision variable associated with the i^{th} sailfish.

To evaluate the quality of each candidate solution, a fitness function is applied to every sailfish position vector. The fitness of the i^{th} sailfish is computed as

$$\text{Fitness of sailfish} = f(SF_1, SF_2, \ldots, SF_m) \tag{26}$$

The fitness values of all sailfish are stored in a fitness vector, which is used to rank and compare candidate solutions throughout the optimization process. The corresponding fitness representation is given by

$$SF_{\text{fitness}} = \begin{bmatrix} f(SF_{1,1}, SF_{1,2}, \ldots, SF_{1,d}) \\ f(SF_{2,1}, SF_{2,2}, \ldots, SF_{2,d}) \\ \vdots \\ f(SF_{m,1}, SF_{m,2}, \ldots, SF_{m,d}) \end{bmatrix} = \begin{bmatrix} F_{SF1} \\ F_{SF2} \\ \vdots \\ F_{SFm} \end{bmatrix} \tag{27}$$

Here, F_{SF_i} denotes the fitness value of the i^{th} sailfish, while SF_{fitness} stores the fitness values of all sailfish in the population. During the evaluation process, each row of the SF_{position} matrix is supplied to the fitness function, and the resulting objective-function value is recorded in the corresponding entry of the SF_{fitness} vector Shadravan et al. [14]. This fitness information is subsequently used to identify the elite sailfish and guide the search toward promising regions of the solution space.

In addition to the sailfish population, the school of sardines plays a fundamental role in the Sailfish Optimization (SFO) algorithm. Similar to sailfish, sardines are assumed to move throughout the search space and contribute to the optimization process by providing alternative candidate solutions [13]. The positions of all sardines are stored in a position matrix defined as

$$S_{position} = \begin{bmatrix} S_{1,1} & S_{1,2} & \ldots & S_{1,d} \\ S_{2,1} & S_{2,1} & \ldots & S_{2,d} \\ \vdots & \vdots & \vdots & \vdots \\ S_{n,1} & S_{n,1} & \ldots & S_{n,d} \end{bmatrix} \tag{28}$$

where n denotes the total number of sardines in the population, d represents the number of decision variables, and $S_{i,j}$ corresponds to the value of the j^{th} decision variable associated with the i^{th} sardine.

The quality of each sardine solution is evaluated using the objective function. The fitness of the i^{th} sardine is computed as

$$S_{\text{position}} = \begin{bmatrix} f(S_{1,1}, S_{1,2}, \ldots, S_{1,d}) \\ f(S_{2,1}, S_{2,2}, \ldots, S_{2,d}) \\ \vdots \\ f(S_{n,1}, S_{n,2}, \ldots, S_{n,d}) \end{bmatrix} = \begin{bmatrix} F_{S1} \\ F_{S2} \\ \vdots \\ F_{Sn} \end{bmatrix} \tag{29}$$

The fitness values of all sardines are stored in a fitness vector given by SF_{fitness} which, stores the fitness values of all sardines in the population. Each row of the S_{position} matrix is evaluated using the objective function, and the resulting fitness value is stored in the corresponding entry of the SF_{fitness} vector.

It is important to note that both sailfish and sardines are essential components of the SFO algorithm. Sailfish act as the primary search agents distributed throughout the search space, whereas sardines contribute additional search information that assists in locating promising regions of the solution space. During the optimization process, sardines may be "captured" by sailfish when they exhibit superior fitness values. In such cases, the sailfish updates its position by adopting the position of the corresponding sardine, thereby replacing a poorer solution with a better one. This predator–prey interaction enhances the search capability of the algorithm and accelerates convergence toward the global optimum [15].

3.2. Elitism

During the optimization process, high-quality solutions may be lost when the positions of search agents are updated, potentially causing the algorithm to converge toward inferior solutions. To address this issue, the SFO algorithm incorporates an elitism mechanism, whereby the best solution identified in the current iteration is preserved and carried forward to subsequent iterations. This strategy ensures that valuable search information is retained throughout the optimization process and prevents the loss of promising candidate solutions.

In SFO, the sailfish with the highest fitness value is designated as the elite sailfish, and its position is stored at every iteration. This elite sailfish represents the best solution discovered thus far and serves as a guiding reference for the movement of other search agents. Inspired by the natural hunting behaviour of sailfish, the elite sailfish influences the manoeuvrability and acceleration of the sardine population during the search process.

Furthermore, during collaborative hunting, some sardines may become injured by the sailfish's rostrum. The position of the best injured sardine is also retained as a valuable source of search information. Let $X^i_{elite\_SF}$ and $X^i_{injured\_S}$, denote the positions of the elite sailfish and the best injured sardine, respectively, at the i^{th} iteration. These two positions represent the most promising solutions among the sailfish and sardine populations and are subsequently used to guide the search process.

By preserving the elite sailfish and injured sardine positions, the SFO algorithm maintains high-quality solutions throughout the optimization process, enhances convergence characteristics, and reduces the likelihood of repeatedly exploring regions associated with previously discarded solutions. Consequently, the elitism mechanism improves both the search efficiency and solution quality of the algorithm.

3.3. Attack-alternation Strategy

Sailfish are known to improve hunting efficiency through an attack–alternation strategy, whereby an individual attacks a prey school only when other members of the group are not actively attacking. During group hunting, sailfish continuously chase and herd their prey while adjusting their positions according to the movements of neighbouring hunters, despite the absence of direct coordination. Inspired by this natural behaviour, the SFO algorithm emulates the attack–alternation mechanism to perform effective exploration of the search space.

As illustrated in Figure 3, the search agents initially execute an exploration phase in which large regions of the search space are investigated to identify promising candidate solutions. Unlike conventional search strategies that move in predefined directions, sailfish in the SFO algorithm can attack from multiple directions within a gradually shrinking search region. Consequently, sailfish update their positions around the best solution found so far. At the i^{th} iteration, the updated position of a sailfish, denoted by $X^i_{new\_SF}$, is determined as

$$X^i_{\text{new\_SF}} = X^i_{\text{elite\_SF}} - \lambda_i \left[\text{rand}(0,1) \left(\frac{X^i_{\text{elite\_SF}} + X^i_{\text{injured\_S}}}{2} \right) \right]. \quad (30)$$

Here, $X^i_{new\_SF}$ represents the updated position of the sailfish at the i^{th} iteration, $X^i_{elite_SF}$ denotes the position of the elite sailfish (the best solution identified thus far), and $X^i_{injured_S}$ corresponds to the position of the best injured sardine. The term $rand(0,1)$ is a uniformly distributed random number in the interval $[0,1]$, while λ_i is an adaptive coefficient that governs the movement of sailfish and is calculated as

$$\lambda_i = 2 \times [rand(0,1)] \times PD - PD \quad (31)$$

The parameter PD represents the prey density, which reflects the relative abundance of prey during the hunting process. As the number of available sardines decreases throughout the search process, the prey density also decreases. Therefore, PD serves as an important adaptive factor for updating sailfish positions around the prey school and is defined as

$$PD = 1 - \left[\frac{N_{SF}}{N_{SF} + N_S} \right] \quad (32)$$

where N_{SF} and N_S denote the numbers of sailfish and sardines, respectively. Since the initial sardine population is generally larger than the sailfish population, the number of sailfish is initialized according to N_{SF} is calculated $N_S \times PP$, where, PP represents the percentage of the sardine population selected to form the initial sailfish population.

The position-update mechanism is based on the average distance between the elite sailfish and the best injured sardine. This strategy enables the algorithm to preserve promising search regions while simultaneously encouraging exploration of new areas through the adaptive coefficient λ_i. Because λ_i varies dynamically according to the prey density, sailfish can either diverge from or converge toward promising regions of the search space. This adaptive behaviour enhances the global exploration capability of the SFO algorithm and improves its ability to avoid premature convergence.

Furthermore, sailfish update their positions through two complementary mechanisms. First, they directly attack the prey school by exploiting information obtained from the elite sailfish and injured sardine. Second, they occupy vacant regions surrounding the prey school, thereby simulating an encirclement strategy. These coordinated search behaviours increase the probability of identifying superior candidate solutions and improve the overall convergence performance of the SFO algorithm [15].

3.4. Sardine Position Update and Attack Power Mechanism

At the beginning of group hunting, sailfish rarely achieve complete capture of sardines. In most cases, the sailfish's bill only removes scales from the sardines, causing injuries to many individuals within the school. During the initial stage of the hunt, sailfish possess sufficient energy to pursue prey effectively, while the sardines remain fresh, uninjured, and capable of maintaining high escape speeds and manoeuvrability. As the hunt progresses, the attacking capability of the sailfish gradually decreases, and the sardines experience fatigue due to repeated attacks. Consequently, their ability to detect predators weakens, reducing the effectiveness of the school's collective escape strategy. Eventually, injured sardines become separated from the school and are captured more easily by the sailfish [15].

To model this behaviour, each sardine updates its position according to the elite sailfish position and the sailfish's attack power during each iteration. In the SFO, the new position of a sardine at the i^{th} iteration is determined as

$$X^i_{new\_S} = r \times \left(X^i_{elite\_SF} - X^i_{old\_S} + AP\right) \quad (33)$$

where $X^i_{SF,\text{elite}}$ denotes the position of the elite sailfish, $X^i_{S,\text{old}}$ represents the current sardine position, r is a uniformly distributed random number in the range $[0, 1]$, and AP denotes the sailfish attack power.

The AP is computed as

$$AP = A \times [1 - (2 \times Itr \times \in)] \quad (34)$$

where A and ε are control parameters responsible for linearly decreasing the AP from A to zero throughout the optimization process.

The influence of the attack strategy can be observed through the possible locations of sardines after a sailfish attack. When attacked, sardines rapidly disperse to evade capture by updating their positions according to the parameters r and AP. The random parameter r controls the degree of dispersion around the predator. This position-update mechanism enables sardines to escape from the elite sailfish while simultaneously gathering information from neighbouring individuals, thereby enhancing local search capability. Consequently, the algorithm maintains an effective balance between exploration and exploitation of the search space [15].

Furthermore, both the number of sardines that update their positions and the extent of their movement depend on the sailfish AP. Since the AP decreases over time, it adaptively guides the convergence behaviour of the search agents. The number of sardines selected for updating (α) and the number of variables updated for each sardine (β) are determined as

$$\alpha = N_S \times AP \quad (35)$$

$$\beta = d_i \times AP \quad (36)$$

where N_S is the total number of sardines and d_i represents the dimensionality of the optimization problem at the i^{th} iteration.

When the AP is low ($AP \leq 0.5$), only α sardines and β variables are updated. In contrast, when the AP is high ($AP > 0.5$), all sardines update their positions. The parameters AP and r introduce additional randomness into the search process, thereby reducing the likelihood of premature convergence and entrapment in local optima.

During the final stage of hunting, injured sardines that become isolated from the school are captured rapidly. In the SFO algorithm, a sardine is considered captured when its fitness becomes superior to that of the corresponding sailfish [15]. In such a case, the sailfish updates its position by replacing it with the position of the captured sardine, as expressed by

$$X^i_{SF} = X^i_S \quad if \quad f(S_i) < f(SF_i) \quad (37)$$

where X^i_S and X^i_{SF} denote the positions of the sardine and sailfish, respectively, at the i^{th} iteration.

Initially, the positions of sailfish and sardines are generated randomly. During each iteration, the position of every sailfish is updated based on the elite sailfish and an injured sardine. Similarly, sardine positions are updated according to the elite sailfish position and the AP mechanism [15]. After updating their positions, all search agents are evaluated using the objective function. If a sardine exhibits better fitness than a sailfish, the sailfish adopts the sardine's position. The positions of both the elite sailfish and the injured sardine are continuously updated throughout the optimization process. Finally, captured sardines are removed from the population. This iterative procedure continues until the termination criterion is satisfied.

3.5. Key Features Contributing to the Global Search Capability of SFO

The SFO possesses several mechanisms that enhance its ability to effectively explore the search space and approximate the global optimum. The major features contributing to its optimization performance are summarized as follows:

1) The random initialization of sailfish and sardine populations promotes extensive exploration of the search space and increases the probability of locating promising regions.
2) The presence of the sardine population helps mitigate premature convergence and reduces the likelihood of stagnation in local optima.
3) The encircling mechanism employed by sailfish creates a hyper-spherical search neighbourhood around potential solutions, thereby enhancing the exploration capability of the algorithm.
4) The manoeuvrability of sardines around the elite sailfish facilitates an effective exploitation process by refining candidate solutions as the optimization progresses.
5) The continuous updating of sardine positions generates diverse movement patterns, increasing the variety of candidate solutions explored in the vicinity of the sailfish population.
6) The gradual reduction of the AP parameter provides a smooth transition from exploration to exploitation, thereby improving the search efficiency.
7) The adaptive decrease in sailfish AP ensures convergence of the algorithm by progressively focusing the search on promising regions of the solution space.
8) The replacement of sailfish positions with fitter sardine positions preserves high-quality solutions and enhances the capability of the algorithm to retain promising search areas during the optimization process.

Collectively, these mechanisms enable the SFO algorithm to maintain an effective balance between global exploration and local exploitation, thereby improving its ability to converge toward the global optimum while avoiding premature convergence.

4. Results and Discussion

4.1. On optimization

The isolated multi-source power system model, as depicted in Figure 1, consists of three Proportional-Integral (PI) controllers whose parameters are optimized using the SFO, as shown in Figure 2. During the optimization process, the parameters of the three controllers are considered as global parameters, denoted as K_{p1}, K_{i1}, K_{p2}, K_{i2}, K_{p3}, and K_{i3}. Among these, K_{p1} and K_{i1} correspond to the common controller, K_{p2} and K_{i2} are associated with the PI controller connected to the thermal source, while K_{p3} and K_{i3} belong to the PI controller connected to the gas source. The population size of the SFO algorithm is set to 30 sailfish and 20 sardines, resulting in a problem dimensionality of 6. The search space for the global parameters is constrained within the range shwon in Table 3 and the maximum number of iterations is set to 100. Upon completion of the optimization process, the optimal parameters obtained using SFO are presented in Table 1 and Table 2, which also includes a comparison of PI controller parameters reported in the literature. For exhaustive analysis and selection of objective function, the system is subjected to application of all six objective functions as mentioned in 2.3 and corresponding results are reported in Table 2. The corresponding fitness function plot with respect to iterations are shown in Figure 3.

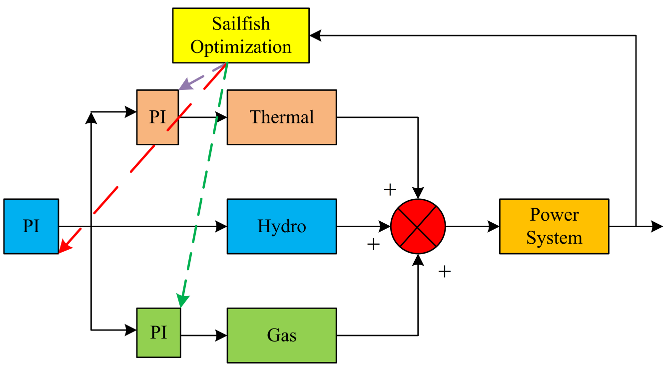

Figure 2. *PI controllers and Optimization using SFO Algorithm.*

The simulation studies are carried out in MATLAB R2018a. The computing platform used for the simulations has the following specifications:

1) Processor: 12th Gen Intel(R) Core(TM) i7-12700H @ 2.30 GHz
2) Installed RAM: 16.0 GB (15.7 GB usable)
3) System Type: 64-bit operating system, x64-based processor
4) Simulation time: 0 - 100 Seconds
5) Type: Variable -step
6) Solver: Auto (Automatic Solver Selection)

4.2. Strengths of the SFO

In the literature, a single-area multi-source power system was considered by Ramakrishna and Bhatti [4]. In this study, three PI controllers were employed for the three generating sources; however, the controllers were not connected individually to each source. Instead, a common PI controller was used, while separate PI controllers were assigned only to the thermal and gas generation units. The present work investigates the application of the Sailfish Optimization (SFO) algorithm for the load frequency control (LFC) of this particular power system. Furthermore, the SFO algorithm can also be employed to optimally tune the parameters of other advanced controllers when applied to different power system configurations and network topologies [4]. The applicability of SFO can be summarized as following:

1) *Good balance between exploration and exploitation:* SFO maintains an effective balance between global search (exploration) and local search (exploitation) through the interaction between sailfish and sardines. This enables the algorithm to explore the search space extensively during the initial iterations and gradually concentrate on promising regions near the optimal solution.
2) *Fast convergence speed:* The algorithm efficiently guides candidate solutions toward better positions, resulting in faster convergence compared with many conventional optimization techniques.
3) *Ability to avoid local minima:* Due to its population-based search mechanism and dynamic predator–prey behavior, SFO reduces the likelihood of becoming trapped in local optima, thereby increasing the probability of obtaining a near-global optimum.
4) *Simple structure and easy implementation:* SFO has a straightforward mathematical formulation and does not require complex operators. Consequently, it is easy to implement in MATLAB and is well suited for solving engineering optimization problems.
5) *Suitable for nonlinear and complex optimization problems:* SFO performs effectively on nonlinear, multimodal, and non-convex optimization problems, where conventional deterministic optimization methods may be ineffective or difficult to apply.
6) *Requires fewer control parameters:* Compared with several other metaheuristic optimization algorithms, SFO requires only a limited number of algorithm-specific control parameters, making parameter tuning easier and reducing implementation complexity.
7) *Improved solution quality:* The cooperative hunting strategy between sailfish and sardines enhances the refinement of candidate solutions, resulting in high-quality optimal or near-optimal solutions.
8) *Robust performance:* SFO exhibits stable performance over repeated runs and has demonstrated effectiveness in a wide range of engineering applications, including controller tuning, feature selection, economic dispatch, and power system optimization.

9) *Effective for controller parameter tuning:* In control and power system applications, SFO is highly effective for tuning PI, PID, and PIDF controller parameters by minimizing error-based objective functions such as IAE, ITAE, ITSE, and ISE.

10) *Applicable to multi-dimensional optimization problems:* SFO can efficiently solve optimization problems involving multiple decision variables, making it suitable for practical engineering systems with numerous unknown parameters.

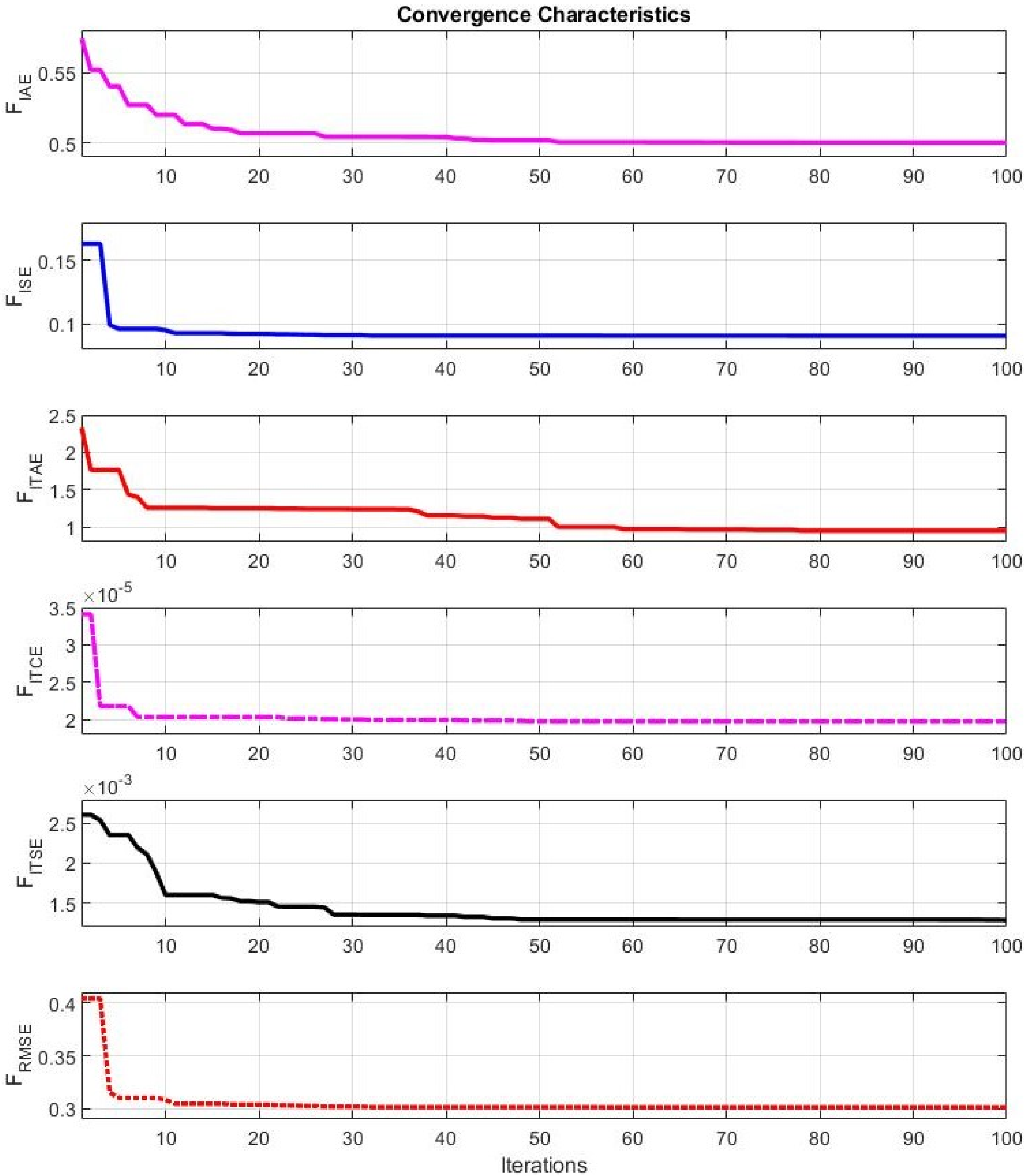

Figure 3. *Fitness functions with respect to iteration for different objective functions.*

The SFO algorithm was selected over Particle Swarm Optimization (PSO) and Grey Wolf Optimization (GWO) because it provides a superior balance between global exploration and local exploitation, which is crucial for optimizing controller parameters in nonlinear interconnected power systems. Unlike PSO, which often converges rapidly but is susceptible to premature convergence and entrapment in local optima, SFO employs a cooperative predator–prey mechanism between sailfish and sardines to enhance search diversity and improve the likelihood of identifying the global optimum. In comparison with GWO, SFO utilizes a more adaptive search strategy by dynamically updating both predator and prey populations, thereby improving convergence characteristics and maintaining population diversity throughout the optimization process. Furthermore, SFO has a simple mathematical formulation, requires fewer algorithm-specific control parameters, and has demonstrated high solution accuracy, robustness, and reliability in solving complex engineering optimization problems. These advantages make SFO a more suitable optimization technique for determining the optimal controller gains in the proposed load frequency control (LFC) system under varying operating conditions.

4.3. Time Domain Analysis

The response of the system in Figure 1 is considered for without controller, controller in literature [4] and with proposed SFO-PI controller. The response of the system without controller is presented in Figure 5 where the steady state error is clearly visible. While, the response of the system with proposed controller and controller in Ramakrishna and Bhatti [4] is presented in Figure 6. To provide a clearer comparison of the system response, the controller parameters optimized using different objective functions are applied to the system, and the corresponding responses are shown in Figure 4.

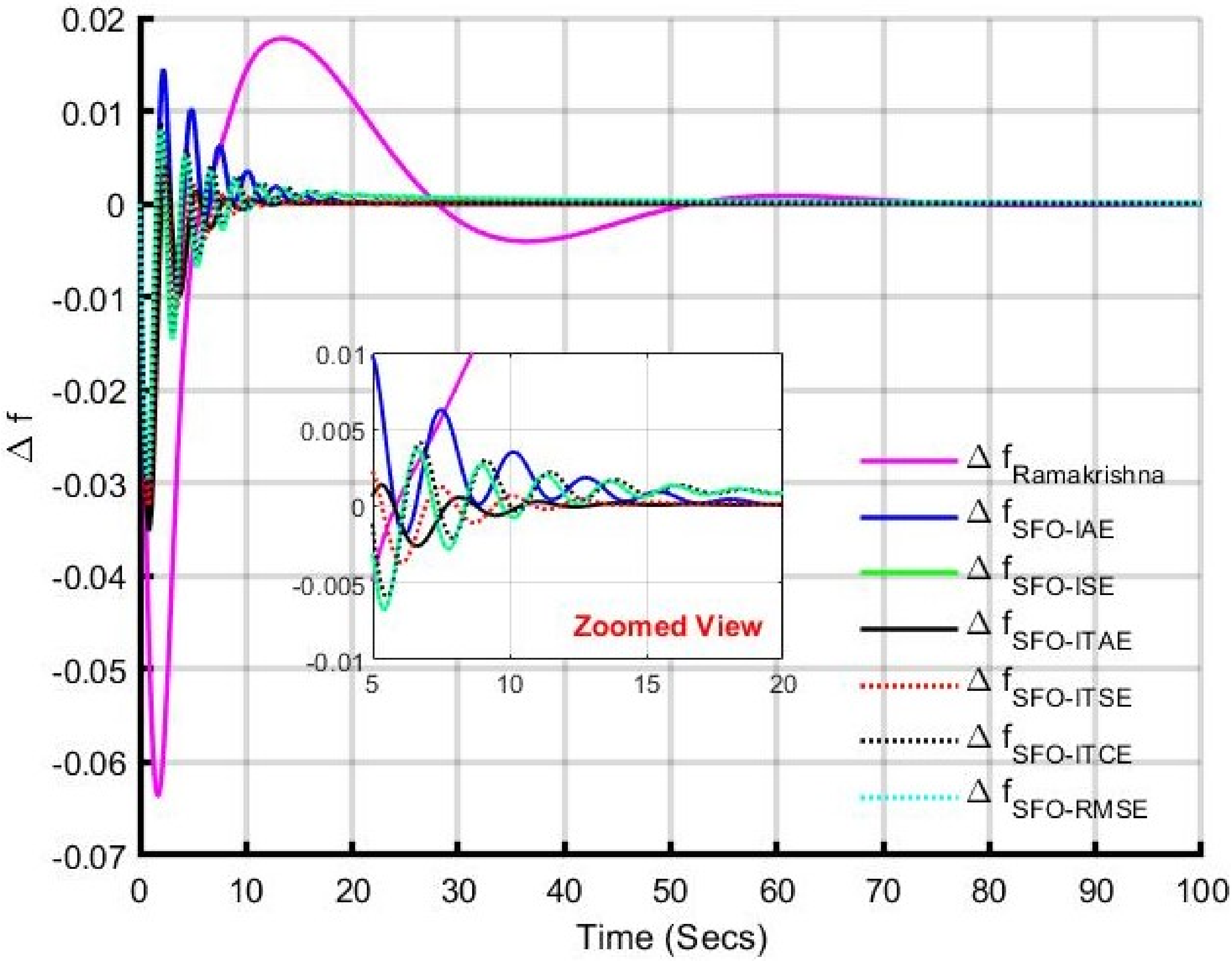

Figure 4. *Response of system frequency with all considered objective functions and compared with the response of the system presented in literature [4].*

Table 1. *Optimal parameters of PI controller.*

Particulars	Common Controller		Controller on Thermal Plant		Controller on Gas Plant	
SFO-PI	0.9543	0.1373	2.0563	0.0103	1.3563	0.2878
Bhatti [4]	0.2051	0.0982	0.3257	0.0929	0.0029	0.1065

Algorithm 1 Sailfish Optimization Algorithm (SFO) [14]

Input: Number of sailfish (N_{SF}), number of sardines (N_S), problem dimension (d), lower bound (lb), upper bound (ub), maximum iterations $(Itr_{\max})$, attack decay coefficient (ε), tolerance (Tol), and stagnation threshold (S_{th}).
Output: Optimal solution (X_{best}) and corresponding fitness value (f_{best}).
Randomly initialize sailfish population within the search bounds.
Randomly initialize sardine population within the search bounds.
Evaluate the fitness of all sailfish and sardines using the objective function.
Identify the elite sailfish and set it as the initial best solution.
Initialize $AP = 1$.
Set stagnation counter $SC = 0$.
for $Itr = 1$ to $Itr_{\max}$ **do**
    Compute prey density based on the current numbers of sailfish and sardines.
    Update the positions of sailfish using the elite sailfish and sardine positions.
    Evaluate the fitness of the updated sailfish population.
    Update the elite sailfish if a better solution is obtained.
    Update the positions of sardines according to the elite sailfish and AP.
    Evaluate the fitness of the updated sardine population.
    Replace inferior sailfish with fitter sardines whenever applicable.
    Update the AP using the predefined decay strategy.
    if $Itr \bmod 10 = 0$ **or** $Itr = Itr_{\max}$ **then**
        Display the current iteration number, best fitness value, and best solution.
    end if
    Check convergence by monitoring the improvement in fitness values.
    if $SC > S_{th}$ **then**
        Print "Stagnation detected".
        break
    end if
    Store the best fitness value and corresponding solution for the current iteration.
end for
Return X_{best} and f_{best}.

Table 2. *Comparison of Different Objective Functions and Optimized PI Parameters.*

S.No	Objective Function	Mathematical Expression	f_{min}	K_{p1}	K_{i1}	K_{p2}	K_{i2}	K_{p3}	K_{i3}
1	Integral of Absolute Error (IAE)	$\int_0^T \lvert e(t)\rvert \, dt$	0.5002	0.9536	0.2854	2.0562	0.2086	0.0254	0.3310
2	Integral of Squared Error (ISE)	$\int_0^T e^2(t) \, dt$	0.0906	0.9543	0.1373	2.0563	0.0103	1.3563	0.2878
3	Integral of Time-Weighted Absolute Error (ITAE)	$\int_0^T t\lvert e(t)\rvert \, dt$	0.9502	0.7767	0.0010	2.0324	0.3044	0.0010	0.4979
4	Integral of Time-Weighted Squared Error (ITSE)	$\int_0^T te^2(t) \, dt$	1.9730	0.9514	0.0010	2.0549	0.3302	0.0010	0.3902
5	Integral of Time-Weighted Cubed Error (ITCE)	$\int_0^T (t\lvert e(t)\rvert)^3 \, dt$	0.0012	0.9542	0.1604	2.0563	0.0100	1.1647	0.3129
6	Root Mean Squared Error (RMSE)	$\sqrt{\frac{1}{N}\sum_{i=1}^{N} e_i^2}$	0.3011	0.9543	0.1373	2.0563	0.0103	1.3563	0.2878

Table 3. *Upper and Lower Bounds of Controller Parameters*

Bounds	K_p1	K_i1	K_p2	K_i2	K_p3	K_i3
Upper Bounds	1.5	1.0	2.5	1.0	2.0	1.0
Lower Bounds	0.01	0.001	0.01	0.01	0.001	0.01

Table 4. *Performance indices of the frequency response using controller parameters tuned with different objective functions and comparison with the literature.*

Method	ISE	IAE	ITAE
SFO-IAE	0.001153752	0.082154412	0.339310055
SFO-ISE	0.000929323	0.096248905	1.395051065
SFO-ITAE	0.001257657	0.066990524	0.398006287
SFO-ITSE	0.001035349	0.063419150	0.338933948
SFO-ITCE	0.000938063	0.093115078	1.188422029
SFO-RMSE	0.000929323	0.096248905	1.395051065
Ramakrishna et al. (2007) [4]	0.011937195	0.486831511	7.139695167

The comparison between the proposed SFO-PI controller and the traditional PI controller in Ramakrishna and Bhatti[4] reveals significant improvements in system performance. The step response analysis indicates that the SFO-PI controller achieves a much faster settling time (27.79 s vs. 47.38 s), nearly reducing it by half, which ensures quicker stabilization of the system. Additionally, the Overshoot is significantly reduced (1.00×10^4 vs 1.44×10^5), indicating a more responsive system. The time domain parameters of the considered responses are enlisted in Table 5.

Further, the performance indices for frequency response of the system using different objective function based controller parameters and comparing with the system parameters in literature, confirm the superiority of the SFO-PI approach as mentioned in Table 4.

Overall, the SFO-PI controller exhibits remarkable improvements in response speed, error minimization, and stability compared to the traditional PI controller. Its ability to reduce settling time, rise time and overshoot and minimize performance errors makes it a superior choice for enhancing frequency stability in multi-source power systems.

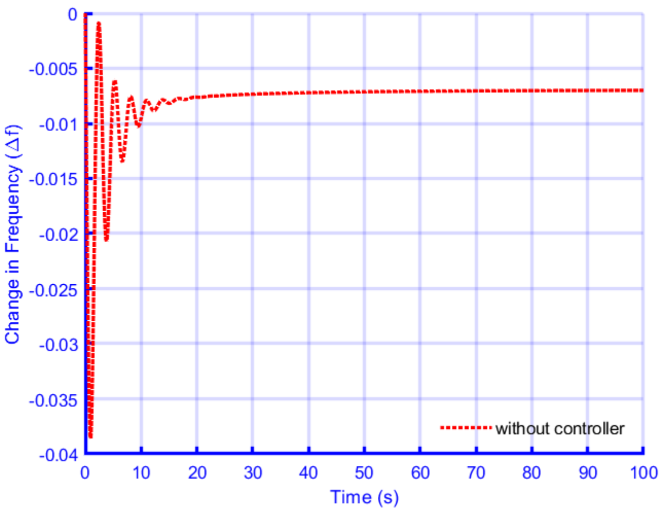

Figure 5. *Response of Isolated Multi-Source Power System Without Controller.*

Table 5. *Comparison of Rise Time, Settling Time, and Overshoot.*

Row	Rise Time	Settling Time	Overshoot
Ramakrishna [4]	2.56×10^{-4}	47.38	1.44×10^6
IAE	1.28×10^{-5}	16.03	2.15×10^6
ISE	0.0019	27.79	1.00×10^4
ITAE	0.0027	7.46	6.99×10^3
ITSE	0.0013	9.14	1.45×10^4
ITCE	0.0014	25.78	1.48×10^4
RMSE	0.0019	27.79	1.00×10^4

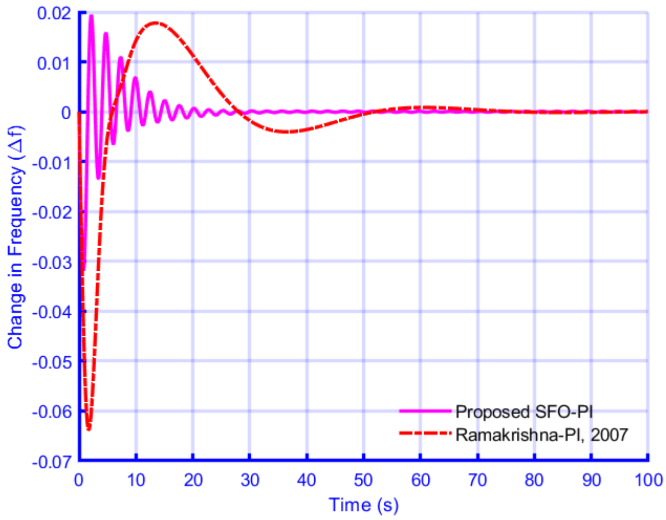

Figure 6. *Response of the isolated multi-source power system with the proposed controller and the controller reported in the literature [4].*

4.4. Eigenvalue Analysis

The comparison of eigenvalues between the PI controller in literature [4] and the proposed SFO-PI controller reveals key insights into system stability and dynamic performance. Both controllers ensure system stability, as all eigenvalues have negative real parts or are zero, confirming that neither approach leads to instability. Importantly, no eigenvalues with positive real parts are observed, which would have indicated an unstable system. The above statement you can verify in the Table 6 and the plot of eigenvalues is shown in Fig 7.

Examining damping characteristics, the traditional PI controller predominantly yields real eigenvalues, indicating a heavily damped system with minimal oscillations. The dominant eigenvalues, which determine the slowest modes of the system, also indicate differences between the two approaches. The SFO-PI controller's dominant eigenvalues have a slightly smaller real part compared to those of the PI controller in literature [4]. Furthermore, some eigenvalues in the proposed controller shift further to the left in the complex plane, suggesting better damping and potentially faster response.

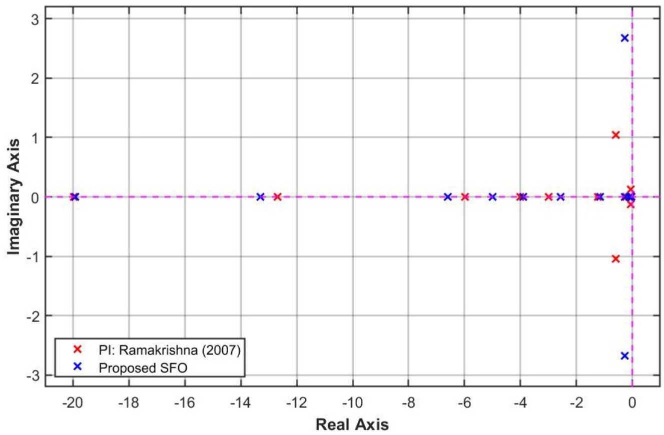

Figure 7. *Eigenvalue Distribution of Ramakrishna and Proposed SFO.*

Table 6. *Eigenvalue Analysis Comparison.*

SFO-PI (Proposed)	PI: Ramakrishna, 2007
$-19.9080 + 0.0000i$	$-19.9785 + 0.0000i$
$-13.3036 + 0.0000i$	$-12.6706 + 0.0000i$
$-6.5872 + 0.0000i$	$-5.9873 + 0.0000i$
$-0.2689 + 2.6818i$	$-5.0000 + 0.0000i$
$-0.2689 - 2.6818i$	$-3.9944 + 0.0000i$
$-3.8942 + 0.0000i$	$-2.9951 + 0.0000i$
$-2.5631 + 0.0000i$	$-0.5755 + 1.0390i$
$-1.1518 + 0.0000i$	$-0.5755 - 1.0390i$
$-0.2714 + 0.0000i$	$-1.2351 + 0.0000i$
$-0.1198 + 0.0000i$	$-0.2278 + 0.0000i$
$-0.0454 + 0.0000i$	$-0.0659 + 0.1299i$
$-0.0209 + 0.0000i$	$-0.0659 - 0.1299i$
$-5.0000 + 0.0000i$	$-0.0313 + 0.0000i$
$0.0000 + 0.0000i$	$-0.0000 + 0.0000i$

In conclusion, the SFO-PI controller offers a better trade-off between stability and dynamic performance. It retains system stability while introducing controlled oscillations that improve transient response. Additionally, it may contribute to a reduction in steady-state error by handling disturbances more effectively. The leftward shift of some eigenvalues further supports the idea of improved damping. However, potential trade-offs include an increase in oscillatory behaviour, which, if not tuned correctly, could lead to unwanted overshoot.Overall, the proposed SFO-PI controller optimally tuned by considering ISE based objective function, appears to enhance performance compared to the PI approach in Ramakrishna and Bhatti [4], making it a more effective choice for improving frequency stability and response characteristics.

The proposed controller eliminates the slow oscillatory mode present in the literature controller, while most of its eigenvalues are shifted further into the left-half of the complex plane, indicating improved stability margins. Furthermore, the slow dynamics of the proposed controller are dominated by real poles, resulting in smoother and less oscillatory system responses.

Although the controller in literature possesses a slightly faster dominant real pole (-0.0313) compared to the proposed ISE controller (-0.0209), it also contains a slow complex-conjugate pole pair located close to the imaginary axis. This lightly damped oscillatory mode adversely affects the transient response. Consequently, considering the overall eigenvalue distribution, the proposed ISE-optimized controller provides improved small-signal stability and transient performance.

Moreover, if the time-domain simulation results (e.g., frequency deviation, settling time, overshoot, and ISE value) also demonstrate improved performance, it can be concluded that the proposed ISE-optimized controller outperforms the conventional PI controller proposed by Ramakrishna and Bhatti [4].

4.5. Dynamic Response under Variable Load Disturbances

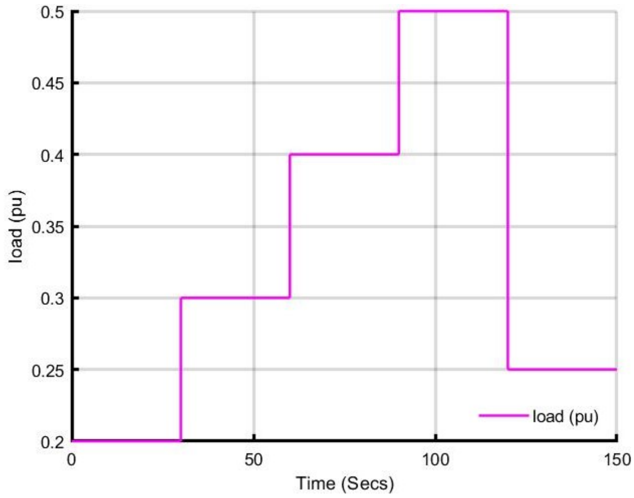

Figure 8. *Varying load.*

To evaluate the robustness of the proposed controller under realistic operating conditions, a variable load profile was applied to the interconnected power system, as illustrated in Figure 8. The load demand was initially maintained at 0.2 p.u. and subsequently changed in a stepwise manner to 0.3 p.u. at $t = 30$ s, 0.4 p.u. at $t = 60$ s, and 0.5 p.u. at $t = 90$ s. Finally, the load was reduced to 0.25 p.u. at $t = 120$ s. This loading sequence represents both incremental and decremental power demand variations commonly encountered in practical power systems.

Figure 9 presents the corresponding frequency deviation (Δf) of the system. It can be observed that each load increment introduces an immediate negative frequency excursion caused by the sudden increase in power demand. Following each disturbance, the controller effectively restores the system frequency toward its nominal value with a well-damped transient response.

At $t = 30$ s, 60 s, and 90 s, the successive increases in load produce similar transient characteristics, demonstrating that the controller maintains satisfactory regulation despite the increasing disturbance magnitude. Although the peak frequency deviation increases with larger load increments, the oscillations decay rapidly after each disturbance, indicating adequate damping and satisfactory small-signal stability.

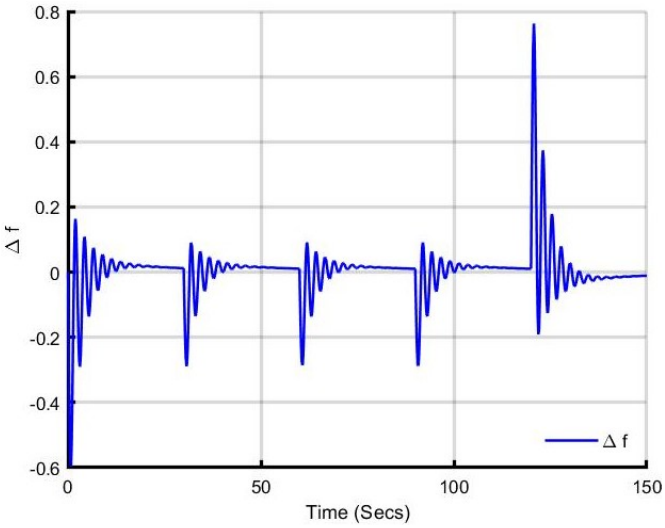

Figure 9. *Frequency response of system with varying load.*

A comparatively larger transient is observed at $t = 120$ s when the load is suddenly reduced from 0.5 p.u. to 0.25 p.u. The abrupt reduction in power demand produces a positive frequency overshoot due to the temporary generation-demand mismatch. Nevertheless, the oscillations are effectively attenuated, and the frequency converges smoothly to its steady-state value without sustained oscillations or instability.

Overall, the obtained results demonstrate that the proposed controller provides stable frequency regulation over a wide range of operating conditions. The controller successfully suppresses frequency oscillations following both load increments and load decrements while maintaining system stability throughout the entire simulation period. The rapid attenuation of oscillations and negligible steady-state frequency error confirm the robustness and effectiveness of the proposed control strategy under continuously varying load conditions.

The proposed control strategy can be further enhanced without modifying the existing decentralized three-PI controller architecture or the Sailfish Optimization (SFO) algorithm. Instead of optimizing the PI controller parameters for a single step load disturbance, the optimization process can be extended to consider multiple operating scenarios or a realistic variable load profile. Such an approach enables the controller to achieve improved robustness and better dynamic performance over a wider range of operating conditions. Furthermore, the objective function may be augmented with an additional term that penalizes oscillatory responses, thereby improving damping characteristics while preserving the simplicity and effectiveness of the existing control structure. This enhancement remains fully consistent with the scope and contributions of the present work and provides a practical means of reducing frequency oscillations under varying load conditions without requiring a complete redesign of the controller.

5. Conclusion

This paper investigated the application of the Sailfish Optimization (SFO) algorithm for optimal tuning of PI controller parameters in a single-area multi-source load frequency control (LFC) system. The effectiveness of the proposed SFO-PI controller was evaluated through dynamic response analysis, performance indices, and eigenvalue assessment.

The simulation results demonstrate that the proposed SFO-PI controller significantly enhances the dynamic performance of the power system compared with the conventional PI controller. The frequency deviations exhibit reduced settling time, lower overshoot, faster transient response, and improved damping characteristics, thereby enabling the system to restore the nominal operating condition more rapidly following load disturbances. Although the optimized controller introduces small oscillations during the transient period, these oscillations are well damped and do not compromise the overall system stability.

The eigenvalue analysis further confirms the improved stability of the proposed controller. All closed-loop eigenvalues remain in the left-half of the complex plane, indicating a stable system. Moreover, the dominant eigenvalues are shifted further toward the left compared to the conventional PI controller, resulting in increased damping and faster decay of oscillations.

Among the investigated objective functions, the Integral of Square Error (ISE) produced the best overall dynamic performance, yielding the lowest frequency deviations and superior transient characteristics. The comparative analysis of different objective functions confirms that appropriate objective function selection plays a crucial role in obtaining optimal controller parameters and achieving enhanced LFC performance.

The superior performance of the proposed approach is primarily attributed to the strengths of the Sailfish Optimization algorithm. SFO effectively balances global exploration and local exploitation, enabling efficient exploration of the search space while avoiding premature convergence to local optima. Its fast convergence speed, robust search capability, and efficient optimization mechanism allow the determination of high-quality controller parameters within fewer iterations, resulting in improved frequency regulation and enhanced system robustness.

Overall, the proposed SFO-PI controller demonstrates superior dynamic response, improved damping, enhanced stability, and lower error indices compared with the conventional PI controller. These findings establish the SFO algorithm as an effective and reliable optimization technique for load frequency control of modern multi-source power systems and highlight its potential for application to more complex interconnected power system networks and advanced controller designs.

ORCID

0009-0004-4800-303X (Shuhangi Sambariya)
0000-0003-1699-0267 (Mahendra Lalwani)
0000-0003-0372-1797 (Dhanesh Kumar Sambariya)

Abbreviations

AGC	Automatic Generation Control
ISE	Integral Square Error
ITAE	Integral of Time-Weighted Absolute Error
ITSE	Integral of Time-Weighted Square Error
IAE	Integral of Absolute Error
ITCE	Integral of Time-Weighted Cubed Error
LFC	Load Frequency Control
LB	Lower Bound
PI	Proportional–Integral
K_p	Proportional Constant
K_i	Integral Constant
PID	Proportional–Integral–Derivative
RMSE	Root Mean Squared Error
SFO	Sailfish Optimization
SFS	Stochastic Fractal Search
SF_{position}	Positions of All Sailfish Solutions Under Optimization
SF_{fitness}	Fitness Values of All Sailfish Under Optimization
S_{position}	Positions of All Sardine Solutions Under Optimization
PD	Prey Density
N_{SF}	Number of Sailfish
N_S	Number of Sardines
PP	Percentage of Sardines Initial Population
λ	Control Parameter That Determines the Prey Density
$X^i_{\text{new\_SF}}$	Updated Position of the Sailfish at the ith Iteration
$X^i_{\text{elite\_SF}}$	Best Position of the Elite Sailfish
$X^i_{\text{injured\_S}}$	Position of the Injured Sardine
AP	Attack Power of Sailfish
α	Sardines' Updated Position Coefficient
β	Number of Variables
UB	Upper Bound

Author Contributions

Mahendra Lalwani: Conceptualization, Investigation, Project administration, Supervision
Dhanesh Kumar Sambariya: Conceptualization, Investigation, Validation
Shuhangi Sambariya: Data curation, Formal analysis, Methodology, Writing – original draft, Writing – review & editing

Conflicts of Interest

The authors declare that they have no known competing financial interests or personal relationships that could have appeared to influence the work reported in this paper.

References

[1] D. K. Sambariya and S. Shringi, "Optimal design of PID controller for load frequency control using harmony search algorithm," *Indonesian Journal of Electrical Engineering and Computer Science*, vol. 5, no. 1, pp. 19-32, 2017. https://doi.org/10.11591/ijeecs.v5.i1.pp19-32

[2] Y. L. Karnavas and E. Nivolianiti, "Harris hawks optimization algorithm for load frequency control of isolated multi-source power generating systems," *International Journal of Emerging Electric Power Systems*, vol. 25, no. 4, pp. 555–571, 2024. https://doi.org/10.1515/ijeeps-2023-0035

[3] D. K. Sambariya, P. Jangid, and S. Sambariya, "Optimal design of load frequency controller for a single area system using fire fly algorithm," in *2023 IEEE Renewable Energy and Sustainable E-Mobility Conference (RESEM)*, 2023, pp. 1–6. https://doi.org/10.1109/RESEM57584.2023.10236160

[4] K. S. S. Ramakrhttpishna and T. S. Bhatti, "Sampled-data automatic load frequency control of a single area power system with multi-source power generation," *Electric Power Components and Systems*, vol. 35, no. 8, pp. 955–980, 2007. https://doi.org/10.1080/15325000701199479

[5] K. Godara and N. Kumar, "Frequency analysis of multi-source single area power system using WCA algorithm," in *2021 4th International Conference on Recent Developments in Control, Automation & Power Engineering (RDCAPE)*, 2021, pp. 492–496. https://doi.org/10.1109/RDCAPE52977.2021.9633690

[6] N. Paliwal, L. Srivastava, and M. Pandit, "Application of grey wolf optimization algorithm for load frequency control in multi-source single area power system," *Evolutionary Intelligence*, vol. 15, no. 1, pp. 563–584, 2022. https://doi.org/10.1007/s12065-020-00530-5

[7] B. K. Sahu, T. K. Pati, J. R. Nayak, S. Panda, and S. K. Kar, "A novel hybrid LUS–TLBO optimized fuzzy-PID controller for load frequency control of multi-source power system," *International Journal of Electrical Power & Energy Systems*, vol. 74, pp. 58–69, 2016.

[8] S. Sambariya, M. Lalwani, and D. K. Sambariya, "Effective design of load frequency controller for a single area system using sailfish optimization algorithm," in *2025 4th OPJU International Technology Conference (OTCON) on Smart Computing for Innovation and Advancement in Industry 5.0*, 2025, pp. 1–8. https://doi.org/10.1109/OTCON65728.2025.11070909

[9] D. Dinakin and P. Oluseyi, "Comparative study of meta-heuristic and classical techniques for automatic generation control of a multi-source single-area hydro-thermal-gas power system," *Kufa Journal of Engineering*, vol. 10, no. 3, pp. 151–172, 2021. https://doi.org/10.30572/2018/KJE/100310

[10] R. Sivalingam, S. Chinnamuthu, and S. S. Dash, "A hybrid stochastic fractal search and local unimodal sampling based multistage PDF plus (1+PI) controller for automatic generation control of power systems," *Journal of the Franklin Institute*, vol. 354, no. 12, pp. 4762–4783, 2017.

[11] S. Padhy, S. Panda, and S. Mahapatra, "A modified GWO technique based cascade PI-PD controller for AGC of power systems in presence of plug in electric vehicles," *Engineering Science and Technology, an International Journal*, vol. 20, no. 2, pp. 427–442, 2017.

[12] Y. L. Karnavas and E. Nivolianiti, "Load frequency control in multi-source power generation systems using Harris hawks optimization algorithm," in *2022 International Conference on Communications, Information, Electronic and Energy Systems (CIEES)*, 2022, pp. 1–6. https://doi.org/10.1109/CIEES55704.2022.9990646

[13] A. Rai and D. K. Das, "Chaotic sailfish optimizer based tilt integral derivative developing controllers to address load frequency control in microgrids with energy storage system," SSRN, 2024. Available: https://ssrn.com/abstract=4967960

[14] S. Shadravan, H. R. Naji, and V. K. Bardsiri, "The sailfish optimizer: A novel nature-inspired metaheuristic algorithm for solving constrained engineering optimization problems," *Engineering Applications of Artificial Intelligence*, vol. 80, pp. 20–34, 2019.

[15] S. M. Azzam, O. E. Emam, and A. S. Abolaban, "An improved differential evolution with sailfish optimizer (DESFO) for handling feature selection problem," *Scientific Reports*, vol. 14, no. 1, p. 13517, 2024. https://doi.org/10.1038/s41598-024-63328-w